



Article

3-Nitroindoles Serving as *N*-Centered Nucleophiles for Aza-1,6-Michael Addition to *para*-Quinone Methides

Jian-Qiang Zhao ^{1,*} , Wen-Jie Wang ¹, Shun Zhou ^{1,2}, Qi-Lin Xiao ¹, Xi-Sha Xue ¹, Yan-Ping Zhang ¹, Yong You ¹, Zhen-Hua Wang ¹  and Wei-Cheng Yuan ^{1,*}

¹ Innovation Research Center of Chiral Drugs, Institute for Advanced Study, Chengdu University, Chengdu 610106, China

² National Engineering Research Center of Chiral Drugs, Chengdu Institute of Organic Chemistry, Chinese Academy of Sciences, Chengdu 610041, China

* Correspondence: zhaojianqiang@cdu.edu.cn (J.-Q.Z.); yuanwc@cioc.ac.cn (W.-C.Y.)

Abstract: An unprecedented *N*-alkylation of 3-nitroindoles with *para*-quinone methides was developed for the first time. Using potassium carbonate as the base, a wide range of structurally diverse *N*-diarylmethylindole derivatives were obtained with moderated to good yields via the protection group migration/*aza*-1,6-Michael addition sequences. The reaction process was also demonstrated by control experiments. Different from the previous advances where 3-nitroindoles served as electrophiles trapping by various nucleophiles, the reaction herein is featured that 3-nitroindoles is defined with latent *N*-centered nucleophiles to react with *ortho*-hydrophenyl *p*-QMs for construction of various *N*-diarylmethylindoles.

Keywords: 3-nitroindoles; *N*-alkylation; *para*-quinone methides; *aza*-1,6-Michael addition; indole derivatives



Citation: Zhao, J.-Q.; Wang, W.-J.; Zhou, S.; Xiao, Q.-L.; Xue, X.-S.; Zhang, Y.-P.; You, Y.; Wang, Z.-H.; Yuan, W.-C. 3-Nitroindoles Serving as *N*-Centered Nucleophiles for Aza-1,6-Michael Addition to *para*-Quinone Methides. *Molecules* **2023**, *28*, 5529. <https://doi.org/10.3390/molecules28145529>

Academic Editor: Gianfranco Favi

Received: 3 July 2023

Revised: 15 July 2023

Accepted: 18 July 2023

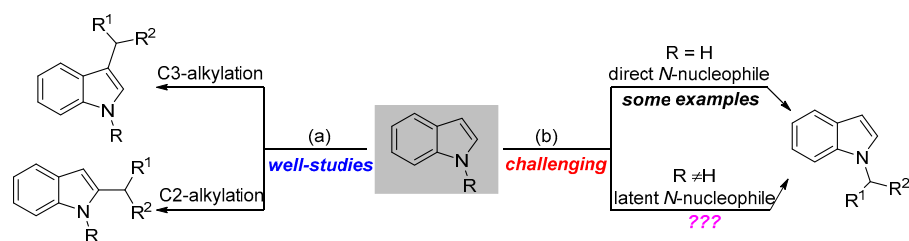
Published: 20 July 2023



Copyright: © 2023 by the authors. Licensee MDPI, Basel, Switzerland. This article is an open access article distributed under the terms and conditions of the Creative Commons Attribution (CC BY) license (<https://creativecommons.org/licenses/by/4.0/>).

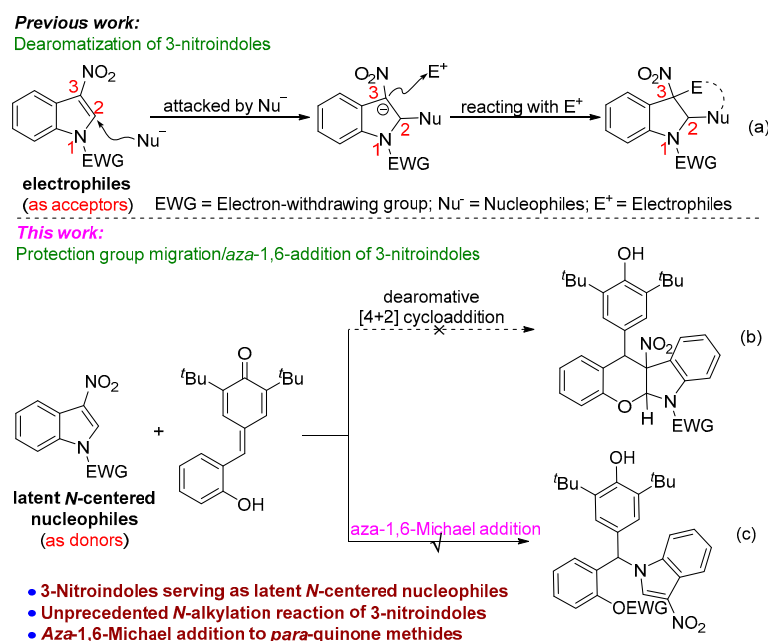
1. Introduction

Indole-based motifs are privileged structures for construction of various valuable complex heteroaromatic units, which widely exist in numerous biologically active natural products and pharmaceutically relevant compounds with potential pharmacological activities, such as against cancer, HIV, inflammation, tuberculosis, hypertension, diabetes, and against microbial, viral, and fungal infections [1–6]. As a result, enormous efforts have been devoted to exploring versatile techniques for the efficient synthesis of structurally diverse indole derivatives, and thus the indole-based chemistry has become a hotspot in organic synthesis [7–12]. In conventional indole alkylation reactions, the most common synthetic modifications occurred at the C2 and C3-positions of indoles due to the innate nucleophilic nature (Scheme 1a) [13,14]. In contrast, the *N*-alkylation of indoles is challenging, and only a few reports have been disclosed to directly fabricate such compounds (Scheme 1b) [15,16]. Among the established *N*-alkylation of indoles, the studies mainly focused on modification of *N*-H indole derivatives by taking advantage of the nucleophilicity of the nitrogen atom [17–23]. However, the weak nucleophilicity of the nitrogen atom in indoles commonly resulted in the C2 or C3-positions alkylated by-products. In order to increase the *N*-centered nucleophilicity, an alternative method is the introduction of a protecting group at the N1-position of indoles made it latent nucleophiles [24–27], which are themselves not nucleophilic but can produce a strong nucleophile in situ via deprotection. To the best of our knowledge, it was only in 2019 that the Vilotijevic group reported that *N*-silyl indoles were employed as latent *N*-centered nucleophiles in the substitution of allylic fluorides for *N*-allyl indoles [28]. Therefore, the exploration of *N*-protected indoles as latent *N*-centered nucleophiles in *N*-alkylation reaction is huge challenges.



Scheme 1. The strategies of direct alkylation of indoles. (a) C2 and C3-alkylation of indoles; (b) N-alkylation of indoles.

In recent years, there have been an increasing number of reports on 3-nitroindoles as electrophiles in the reaction with various nucleophiles for the construction of diverse indolines via dearomative process [29–33]. Among these reactions, 3-nitroindoles are characterized by their readiness to be attacked by nucleophiles at the C2-position and sequentially trapped by electrophiles with the C3-position for the synthesis of indoline-containing polycyclic compounds (Scheme 2a). On the other hand, we have noticed that in the field of *para*-quinone methides (*p*-QMs) chemistry [34–37], *ortho*-hydrophenyl *p*-QMs have been used as donors to trigger some cycloaddition reactions with electron-deficient 2π -components, providing an access to chromans with structural diversity [38–44]. Along this line, as well as our continuing efforts on the dearomatization of nitroheteroarenes [45–48], we conceived that the dearomative [4 + 2] cycloaddition of electron-deficient 3-nitroindoles and *ortho*-hydrophenyl *p*-QMs might occur via the tandem *oxy*-Michael addition/1,6-addition under alkaline conditions (Scheme 2b) [49]. To our surprise, the reaction between 3-nitroindoles and *ortho*-hydrophenyl *p*-QMs did undergo smoothly but providing unanticipated *N*-alkylation products via protection group migration/*aza*-1,6-Michael addition pathway instead of the dearomative [4 + 2] cyclo-adducts (Scheme 2c). In this manuscript, the *N*-protected 3-nitroindoles served as latent *N*-centered nucleophiles to couple with *ortho*-hydrophenyl *p*-QMs and the protecting group was transferred from the *N*-center of indoles to the *O*-center of *ortho*-hydrophenyl *p*-QMs, leading to the *N*-diarylmethylindoles with good yields. Obviously, different from the previous advances where 3-nitroindoles serving as electrophiles were attacked by various nucleophiles, the reaction herein is featured that 3-nitroindoles is defined with latent *N*-centered nucleophiles to react with *ortho*-hydrophenyl *p*-QMs. Herein, we wish to report the initial finds toward this protection group migration/*aza*-1,6-Michael addition sequences.



Scheme 2. The profile of dearomatization of 3-nitroindoles and this work on unprecedented *N*-

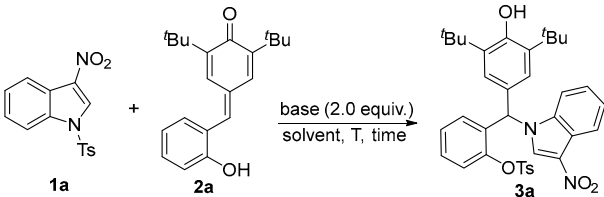
alkylation of 3-nitroindoles. (a) The reaction feature of 3-nitroindoles; (b) The expected dearomatic [4 + 2] cycloaddition of 3-nitroindoles; (c) The unanticipated *N*-alkylation of 3-nitroindoles in this work.

2. Results and Discussion

2.1. Optimization Studies

We started our research with the selection of *N*-Ts 3-nitroindole **1a** and *ortho*-hydroxyphenyl-substituted *para*-quinone methide **2a** as the model substrates for optimizing the reaction conditions (Table 1). Using 1,4-diazabicyclo[2.2.2]octane (DABCO) as the base, the desired *N*-alkylated product **3a** was obtained in 44% yield in toluene at 50 °C for 7 days (entry 1). However, when DABCO was replaced with stronger organic base 1,8-diazabicyclo[5.4.0]undec-7-ene (DBU), a reduced yield was observed (entry 2). We then tested different inorganic bases such as Na₂CO₃ and K₂CO₃ (entries 3 and 4), and it was found that K₂CO₃ was the best candidate, giving the product **3a** with a yield of 60% (entry 4). Afterward, various solvents including CH₂Cl₂, THF, EtOAc, CH₃CN and MeOH were examined, and it was found that CH₃CN was the best choice to give the product **3a** in 67% yield (entry 8 vs. entries 5–7 and 9). By cooling the reaction temperature to room temperature (rt), the yield of **3a** could be increased to 71% (entry 10). A slightly lower yield was obtained when the amount of K₂CO₃ was reduced to 1.0 equivalent (entry 11). Though a series of detailed investigations, the reaction conditions were eventually optimized as follows: 1.0 mmol of **1a** and 1.0 mmol of **2a**, 2.0 equiv. of K₂CO₃ as base in CH₃CN as solvent at room temperature.

Table 1. Optimization of reaction conditions [a].



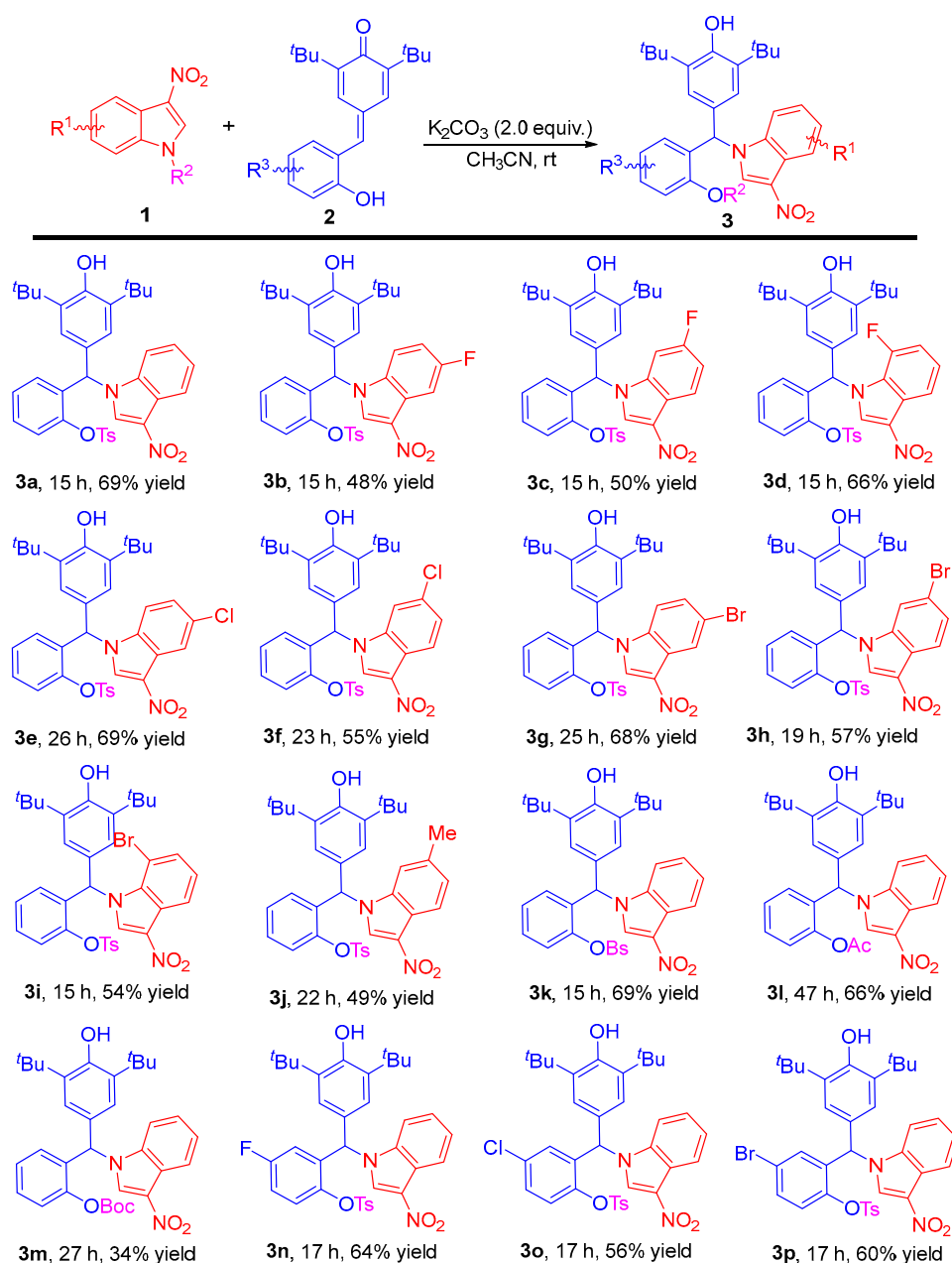
Entry	Base	Solvent	T (°C)	Time (h)	Yield [b]
1	DABCO	toluene	50	168	44
2	DBU	toluene	50	68	24
3	Na ₂ CO ₃	toluene	50	145	trace
4	K ₂ CO ₃	toluene	50	26	60
5	K ₂ CO ₃	CH ₂ Cl ₂	50	88	57
6	K ₂ CO ₃	THF	50	63	58
7	K ₂ CO ₃	EtOAc	50	136	63
8	K ₂ CO ₃	CH ₃ CN	50	23	67
9	K ₂ CO ₃	MeOH	50	20	19
10	K ₂ CO ₃	CH ₃ CN	rt	23	71
11 [c]	K ₂ CO ₃	CH ₃ CN	rt	48	64

[a] Unless otherwise noted, the reaction was carried out with **1a** (0.05 mmol), **2a** (0.05 mmol), and base (2.0 equiv.) in 0.5 mL of solvent at indicated temperature for specified time. [b] Isolated yield. [c] 1.0 equiv K₂CO₃ was used.

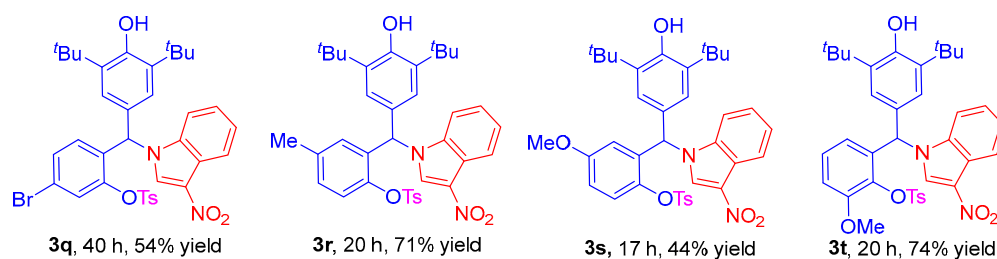
2.2. Substrate Scope Studies

With the optimal reaction conditions in hand, we next surveyed the scope and generality for the *N*-alkylation of 3-nitroindoles with *para*-quinone methides. As shown in Scheme 3, by installing a fluorine atom into the aromatic ring at the C5-, C6- or C7-position of *N*-Ts-3-nitroindoles, these reactions proceeded well to provide the corresponding products **3b–d** in moderate yields. Moreover, 3-nitroindoles bearing different electron-withdrawing group, such as Cl- and Br-, regardless of their position on the aromatic ring,

could react smoothly with **2a** to deliver products **3e–i** in satisfactory results. Nevertheless, the 3-nitroindole bearing a methyl group on the aromatic ring was also viable under the standard conditions, as demonstrated by the formation of product **3j** in 49% yield. Changing the *N*1-protecting group of 3-nitroindole from -Ts to -Bs, had little effect on the reactivity, which could react smoothly with *ortho*-hydroxyphenyl-substituted *para*-quinone methide **2a**, providing the corresponding product **3k** in 69% yield. In addition, the developed catalytic system was also compatible with the *N*-Ac and *N*-alkoxycarbonylated protected 3-nitroindoles, generating the desired products **3l** and **3m** in acceptable yields via tandem protection group migration/*aza*-1,6-Michael addition sequences. On the other hand, various *ortho*-hydroxy *p*-QMs with either electron-withdrawing or -donating groups in the phenyl ring irrespective of their position were well tolerated to provide the expected products **3n–t** in moderate to good yields.



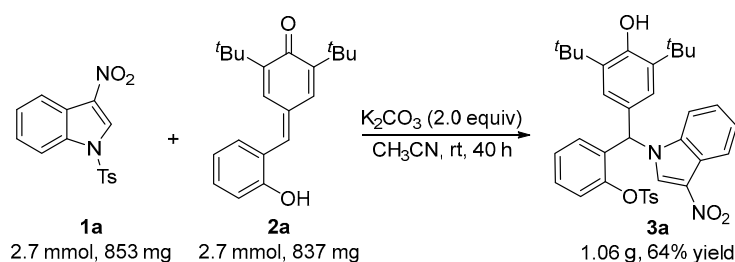
Scheme 3. Cont.



Scheme 3. Substrate scope of *ortho*-hydroxy *p*-QMs and 3-nitroindoles. Reaction conditions: the reactions were carried out with **1** (0.1 mmol), **2** (0.1 mmol) and K_2CO_3 (2.0 equiv) in 1.0 mL of CH_3CN at room temperature. The yield refers to the isolated yield.

2.3. Scale-Up Experiment

To demonstrate the synthetic potential of this unprecedented *N*-alkylation of 3-nitroindoles and *para*-quinone methides, a scale-up experiment was performed between **1a** and **2a**, which is 27 times larger than the scale of the model reaction in Scheme 3. As shown in Scheme 4, the gram-scale reaction proceeded well under the standard conditions and afforded the desired product **3a** in 64% yield, suggesting that the developed protocol has good scalability in organic synthesis.

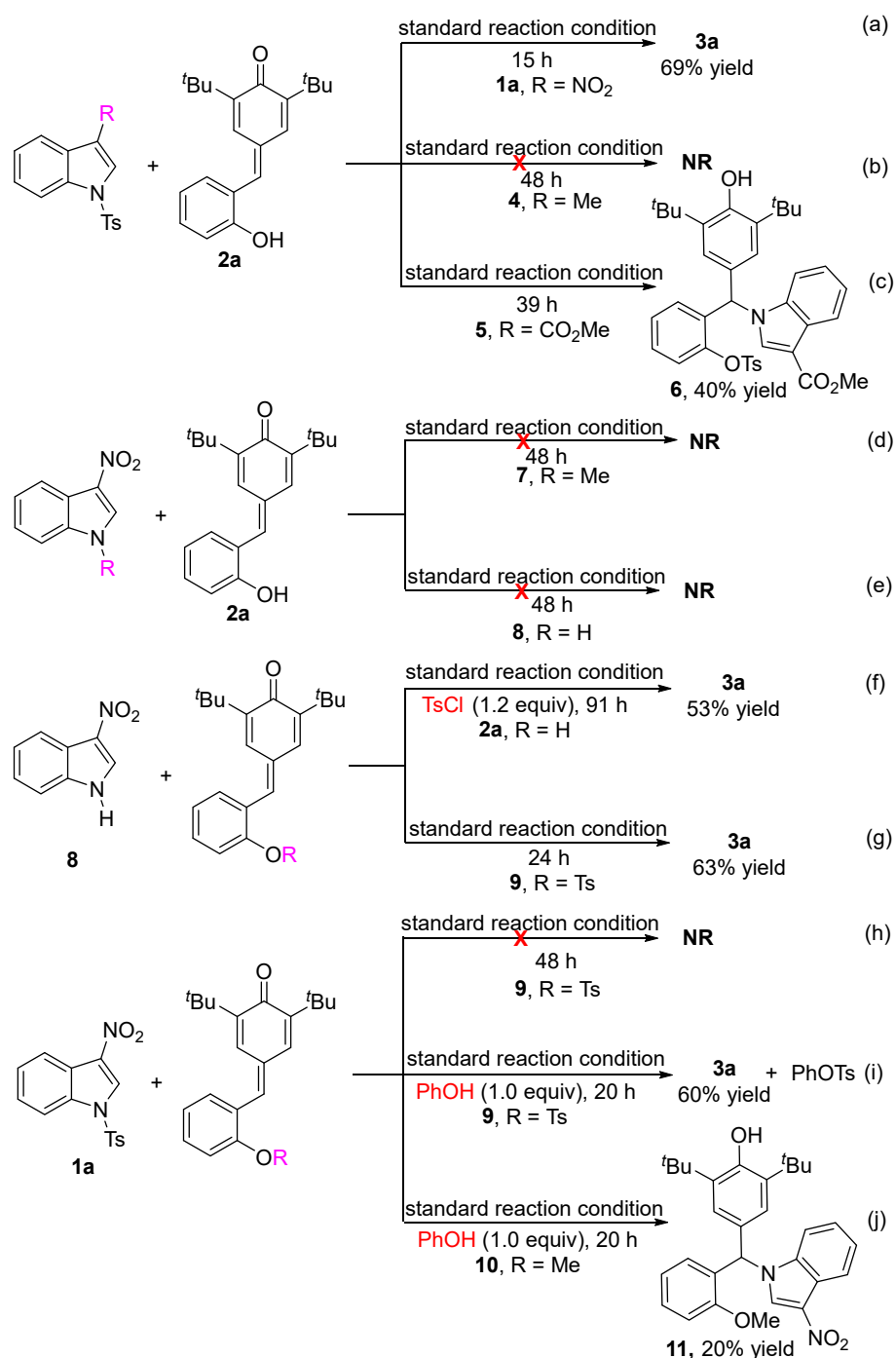


Scheme 4. Scale-up experiment.

2.4. Control Experiments

In order to clarify the possible reaction mechanism, some control experiments were carried out (Scheme 5). The reaction of **1a** and **2a** provided the desired *N*-alkylated product **3a** in 69% yield under the standard reaction conditions (Scheme 5a). Changing the nitro group of **1a** to methyl resulted in the substrate **4** being formed, which failed to react with **2a** (Scheme 5b). When the *N*-Ts indole-3-carboxylate **5** was reacted with **2a**, the reaction gave the corresponding product **6** in 40% yield (Scheme 5c). These experimental results show that the installation of an electron-withdrawing group at the C3-position of indole is crucial for this *aza*-1,6-Michael addition. Furthermore, the effect of the *N*1-protecting group of 3-nitroindole on the reactivity was also investigated (Scheme 5d,e). With the electron-donating group *N*-Me 3-nitroindole **7** or *N*-H 3-nitroindole **8** as the substrate, no desired *N*-alkylated product was detected (Scheme 5d,e). Comparing the results with Scheme 5a, it can be concluded that the *N*1-electron-withdrawing group of indoles plays an important role in assisting migration of *N*-electron-withdrawing group of 3-nitroindoles to *O*-center of *ortho*-hydroxyphenyl *p*-QMs and forming the *N*-centered nucleophiles. In addition, it was found that the one-pot reaction of *N*-H 3-nitroindole **8**, **2a** and TsCl could give product **3a** in 53% yield (Scheme 5f), and the reaction of *N*-H 3-nitroindole **8** and *ortho*-OTs *p*-QM **9** could also afford **3a** in 63% yield (Scheme 5g). From these two reactions, it can be confirmed that the sulfonylation of *ortho*-hydroxy *p*-QMs could enhance the electrophilicity and facilitate subsequent *aza*-1,6-Michael addition. Moreover, the reaction of *N*-Ts-3-nitroindole **1a** and *ortho*-OTs *p*-QM **9** could not happen under the standard reaction conditions (Scheme 5h). However, by adding 1.0 equivalent PhOH into the reaction system, the reaction was able to give **3a** in 60% yield, together with the formation of PhOTs (Scheme 5i). Meanwhile, the three-component reaction of **1a**, *ortho*-OMe *p*-QM **10** and PhOH also proceeded to give product **11** and PhOTs (Scheme 5j). These control experiments show that the *N*-EWG of **1a**

is first transferred to *O*-EWG of **2a** to form **9** under alkaline condition, and then the *aza*-1,6-Michel addition to *para*-quinone methides takes place to give the *N*-alkylated products.

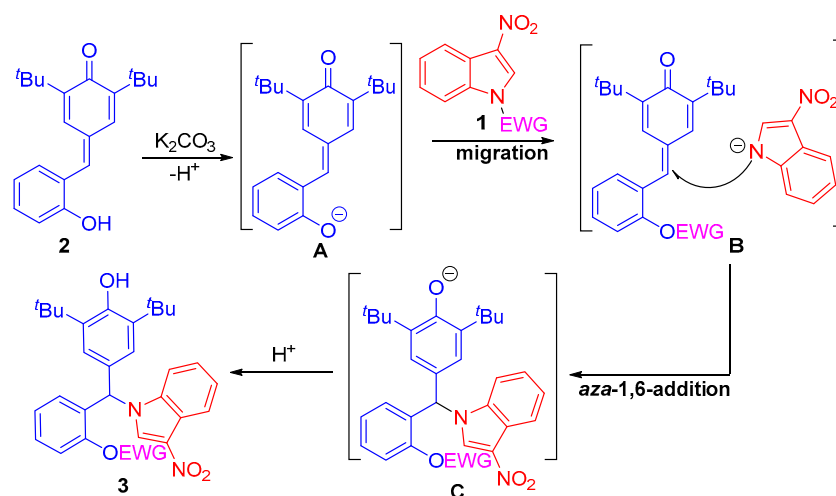


Scheme 5. Control experiments.

2.5. Plausible Reaction Mechanism

Based on our experimental results and the above control experiments, a plausible reaction mechanism was proposed for this base-mediated *N*-alkylation of 3-nitroindoles with *para*-quinone methides. As shown in Scheme 6, the initially K₂CO₃-promoted deprotonation of *ortho*-hydroxy phenyl *p*-QMs **2** affords intermediate **A**. Then the protecting group was transferred from the *N*-center of indoles to the *O*-center of *ortho*-hydroxyphenyl *p*-QMs to give *ortho*-OEWG phenyl *p*-QMs and the 3-nitroindole anion intermediates **B**, which

undergoes an *aza*-1,6-Michael addition to give the intermediate C. Finally, the protonation of intermediate C gives rise to the formation of the *N*-alkylated products 3.



Scheme 6. Plausible reaction mechanism.

2.6. X-ray Crystallographic Structures

All the *N*-alkylation products obtained from the reaction of 3-nitroindoles with *ortho*-hydrophenyl *p*-QMs were unambiguously characterized by nuclear magnetic resonance spectroscopy and high resolution mass spectroscopy. Nevertheless, the structures of products **3l** and **3p** were confirmed by X-ray crystallographic study of the single crystals, which could be readily prepared from the mixture solvents of dichloromethane/EtOH (V:V = 1/10) at room temperature by slow evaporation of solvents (Figure 1). CCDC-2268774 (**3l**) and CCDC-2268775 (**3p**) contain the supplementary crystallographic data for this paper, which can be obtained free of charge from The Cambridge Crystallographic Data Centre.

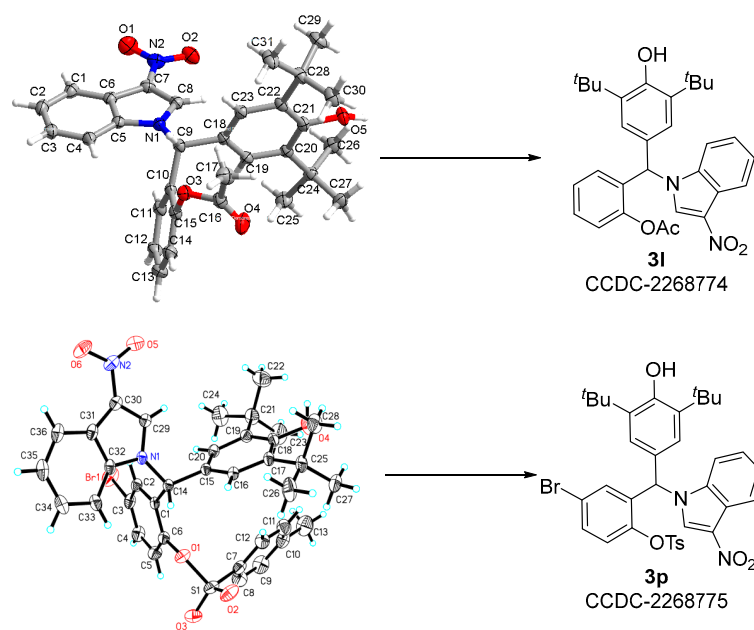


Figure 1. X-ray crystallographic structures of **3l** and **3p**.

3. Materials and Methods

3.1. General Information

Reagents were purchased from commercial sources and were used as received unless mentioned otherwise. Reactions were monitored by thin layer chromatography (TLC). ^1H NMR and ^{13}C NMR spectra were recorded in CDCl_3 and $\text{DMSO}-d_6$. ^1H NMR chemical shifts are reported in ppm relative to tetramethylsilane (TMS) with the solvent resonance employed as the internal standard (CDCl_3 at 7.26 ppm, $\text{DMSO}-d_6$ at 2.50 ppm). Data are reported as follows: chemical shift, multiplicity (s = singlet, br s = broad singlet, d = doublet, t = triplet, q = quartet, m = multiplet), coupling constants (Hz), and integration. ^{13}C NMR chemical shifts are reported in ppm from tetramethylsilane (TMS) with the solvent resonance as the internal standard (CDCl_3 at 77.20 ppm, $\text{DMSO}-d_6$ at 39.52 ppm). Melting points products were recorded on a Büchi Melting Point B-545. The HRMS were recorded by The HRMS were recorded by Agilent 6545 LC/Q-TOF mass spectrometer.

3.2. General Experimental Procedure for the N-Alkylation of 3-Nitroindoles with para-Quinone Methides for the Synthesis of N-Diarylmethylindole Derivatives 3 (Scheme 3)

In a reaction tube equipped with a magnetic stirring bar, the 3-nitroindoles **1** (0.1 mmol, 1 equiv), *ortho*-hydroxyphenyl-substituted para-quinone methide **2** (0.1 mmol, 1.0 equiv), K_2CO_3 (0.2 mmol, 2.0 equiv) and acetonitrile (1.0 mL) were added. Then, the mixture was stirred at room temperature. After completion, the mixture was concentrated and purified by flash chromatography on silica gel to give the corresponding products **3**.

3a, white solid, 41.8 mg, 69% yield; m.p. 199.5–200.8 °C; ^1H NMR (400 MHz, Chloroform-*d*) δ 8.34–8.27 (m, 1 H), 7.70 (s, 1 H), 7.69–7.64 (m, 2 H), 7.43–7.26 (m, 4 H), 7.26–7.17 (m, 4 H), 7.07 (s, 1H), 6.80 (s, 2 H), 6.71 (dd, J = 7.8, 1.7 Hz, 1 H), 5.33 (s, 1 H), 2.42 (s, 3H), 1.33 (s, 18H). ^{13}C NMR (101 MHz, Chloroform-*d*) δ 154.3, 147.2, 145.9, 136.7, 135.6, 132.7, 132.0, 130.0, 129.9, 129.9, 128.8, 128.5, 128.1, 127.4, 126.2, 125.4, 124.7, 124.5, 122.4, 121.4, 120.7, 112.2, 60.0, 34.4, 30.1, 21.7. HRMS (ESI-TOF) calcd. for $\text{C}_{36}\text{H}_{38}\text{N}_2\text{O}_6\text{SNa}$ [$\text{M} + \text{Na}$] $^+$ 649.2343; found: 649.2357.

3b, white solid, 30.9 mg, 48% yield; m.p. 194.4–195.1 °C; ^1H NMR (400 MHz, Chloroform-*d*) δ 7.96 (dd, J = 9.1, 2.5 Hz, 1H), 7.76–7.62 (m, 3H), 7.38–7.15 (m, 6H), 7.10–6.94 (m, 2H), 6.81 (s, 2H), 6.69 (dd, J = 7.8, 1.7 Hz, 1H), 5.35 (s, 1H), 2.44 (s, 3H), 1.33 (s, 18H). ^{13}C NMR (101 MHz, Chloroform-*d*) δ 160.6 (d, J = 241.4 Hz), 154.4, 147.2, 146.0, 136.8, 132.6, 132.0, 131.9, 131.0, 130.0, 130.0, 128.4, 128.1, 127.5, 125.9, 125.3, 122.5, 122.2, 122.1, 113.6, 113.5 (d, J = 6.8 Hz), 113.2, 106.4 (d, J = 26.4 Hz), 60.4, 34.4, 30.1, 21.7. HRMS (ESI-TOF) calcd. for $\text{C}_{36}\text{H}_{37}\text{FN}_2\text{O}_6\text{SNa}$ [$\text{M} + \text{Na}$] $^+$ 667.2249; found: 667.2261.

3c, white solid, 32.2 mg, 50% yield; m.p. 190.1–191.4 °C; ^1H NMR (400 MHz, Chloroform-*d*) δ 8.24 (dd, J = 8.8, 5.3 Hz, 1H), 7.73–7.66 (m, 3H), 7.43–7.10 (m, 6H), 7.03 (dd, J = 9.3, 2.3 Hz, 1H), 6.94 (s, 1H), 6.80 (s, 2H), 6.69 (dd, J = 7.7, 1.7 Hz, 1H), 5.35 (s, 1H), 2.44 (s, 3H), 1.34 (s, 18H). ^{13}C NMR (101 MHz, Chloroform-*d*) δ 160.7 (d, J = 243.2 Hz), 154.4, 147.3, 146.0, 136.8, 135.7, 135.3, 132.6, 131.7, 130.3 (d, J = 2.7 Hz), 130.0, 128.8, 128.4, 128.2, 127.5, 125.8, 125.3, 122.6, 122.0 (d, J = 9.8 Hz), 117.8, 113.2 (d, J = 24.4 Hz), 99.0 (d, J = 27.1 Hz), 60.3, 34.4, 30.1, 21.7. HRMS (ESI-TOF) calcd. for $\text{C}_{36}\text{H}_{37}\text{FN}_2\text{O}_6\text{SNa}$ [$\text{M} + \text{Na}$] $^+$ 667.2249; found: 667.2257.

3d, white solid, 42.5 mg, 69% yield; m.p. 192.7–193.7 °C; ^1H NMR (400 MHz, Chloroform-*d*) δ 8.06 (dd, J = 8.1, 1.0 Hz, 1H), 7.65 (s, 1H), 7.58–7.51 (m, 2H), 7.49 (dd, J = 8.2, 1.3 Hz, 1H), 7.39 (td, J = 8.3, 7.9, 1.7 Hz, 1H), 7.28 (s, 1H), 7.28 (td, J = 8.1, 4.5 Hz, 1 H), 7.22 (td, J = 7.6, 1.3 Hz, 1H), 7.18–7.11 (m, 2H), 7.00–6.91 (m, 1H), 6.74 (dd, J = 7.8, 1.7 Hz, 1H), 6.72 (s, 2H), 5.31 (s, 1H), 2.37 (s, 3H), 1.32 (s, 18H). ^{13}C NMR (101 MHz, Chloroform-*d*) δ 154.2, 146.7 (d, J = 225.5 Hz), 136.5, 132.8, 131.2, 130.6, 130.2, 129.8, 129.3, 128.9, 127.9, 126.9, 125.0, 124.9, 124.6, 123.8, 121.7, 116.6, 116.6, 110.7, 110.6, 61.7 (d, J = 7.0 Hz), 34.3, 30.1, 21.7. HRMS (ESI-TOF) calcd. for $\text{C}_{36}\text{H}_{37}\text{FN}_2\text{O}_6\text{SNa}$ [$\text{M} + \text{Na}$] $^+$ 667.2249; found: 667.2258.

3e, white solid, 45.5 mg, 69% yield; m.p. 174.9–175.4 °C; ^1H NMR (400 MHz, Chloroform-*d*) δ 8.29 (d, J = 2.0 Hz, 1H), 7.72–7.64 (m, 3H), 7.38–7.15 (m, 8H), 7.04 (s, 1H), 6.80 (s, 2H), 6.68 (dd, J = 7.8, 1.7 Hz, 1H), 5.36 (s, 1H), 2.44 (s, 3H), 1.33 (s, 18H). ^{13}C NMR (101 MHz,

Chloroform-*d*) δ 154.5, 147.1, 146.0, 136.8, 133.9, 132.6, 131.8, 130.8, 130.7, 130.1, 130.0, 128.4, 128.2, 128.1, 127.5, 125.8, 125.3, 125.3, 122.5, 122.3, 120.3, 113.4, 60.4, 34.4, 30.1, 21.8. HRMS (ESI-TOF) calcd. for $C_{36}H_{37}ClN_2O_6SNa$ $[M + Na]^+$ 683.1953; found: 683.1972.

3f, white solid, 436.4 mg, 55% yield; m.p. 234.8–236.0 °C; 1H NMR (400 MHz, Chloroform-*d*) δ 8.21 (d, J = 8.6 Hz, 1H), 7.75–7.65 (m, 3H), 7.44–7.13 (m, 8H), 6.97 (s, 1H), 6.78 (s, 2H), 6.69 (dd, J = 7.8, 1.7 Hz, 1H), 5.36 (s, 1H), 2.44 (s, 3H), 1.34 (s, 18H). ^{13}C NMR (101 MHz, Chloroform-*d*) δ 154.5, 147.2, 146.0, 136.8, 135.9, 132.6, 131.6, 130.8, 130.4, 130.2, 130.0, 128.8, 128.5, 128.2, 127.5, 125.8, 125.2, 125.2, 122.7, 121.6, 119.8, 112.2, 60.2, 34.4, 30.1, 21.8. HRMS (ESI-TOF) calcd. for $C_{36}H_{37}ClN_2O_6SNa$ $[M + Na]^+$ 683.1953; found: 683.1965.

3g, white solid, 47.9 mg, 68% yield; m.p. 238.4–239.7 °C; 1H NMR (400 MHz, Chloroform-*d*) δ 8.46 (d, J = 1.9 Hz, 1H), 7.67 (d, J = 9.0 Hz, 3H), 7.42–7.30 (m, 2H), 7.30–7.13 (m, 6H), 7.04 (s, 1H), 6.80 (s, 2H), 6.68 (dd, J = 7.7, 1.6 Hz, 1H), 5.36 (s, 1H), 2.44 (s, 3H), 1.33 (s, 18H). ^{13}C NMR (101 MHz, Chloroform-*d*) δ 154.5, 147.1, 146.0, 136.8, 134.2, 132.6, 131.7, 130.6, 130.1, 130.0, 128.4, 128.1, 128.0, 127.9, 127.5, 125.8, 125.3, 123.4, 122.7, 122.5, 118.4, 113.7, 60.4, 34.4, 30.1, 21.8. HRMS (ESI-TOF) calcd. for $C_{36}H_{37}BrN_2O_6SNa$ $[M + Na]^+$ 729.1434; found: 729.1445.

3h, white solid, 40.1 mg, 57% yield; m.p. 202.6–203.9 °C; 1H NMR (400 MHz, Chloroform-*d*) δ 8.16 (d, J = 8.6 Hz, 1H), 7.74–7.65 (m, 3H), 7.58 (d, J = 1.6 Hz, 1H), 7.50 (dd, J = 8.6, 1.6 Hz, 1H), 7.35 (td, J = 7.8, 1.7 Hz, 1H), 7.28 (d, J = 8.2 Hz, 2H), 7.26–7.16 (m, 2H), 6.98 (s, 1H), 6.78 (s, 2H), 6.70 (dd, J = 7.8, 1.7 Hz, 1H), 5.36 (s, 1H), 2.44 (s, 3H), 1.34 (s, 18H). ^{13}C NMR (101 MHz, Chloroform-*d*) δ 154.5, 147.2, 146.0, 136.8, 136.2, 132.6, 131.6, 130.3, 130.2, 130.0, 128.8, 128.5, 128.2, 127.8, 127.5, 125.8, 125.2, 122.7, 122.0, 120.1, 118.4, 115.2, 60.2, 34.4, 30.1, 21.8. HRMS (ESI-TOF) calcd. for $C_{36}H_{37}BrN_2O_6SNa$ $[M + Na]^+$ 729.1434; found: 729.1442.

3i, white solid, 38.0 mg, 54% yield; m.p. 230.2–231.1 °C; 1H NMR (400 MHz, Chloroform-*d*) δ 8.03 (d, J = 8.1 Hz, 2H), 7.75–7.68 (m, 2H), 7.43–7.32 (m, 3H), 7.17–7.08 (m, 3H), 7.08–6.92 (m, 3H), 6.87 (td, J = 7.4, 1.3 Hz, 1H), 5.22 (s, 1H), 4.97 (s, 1H), 2.46 (s, 3H), 1.39 (s, 18H). ^{13}C NMR (101 MHz, Chloroform-*d*) δ 153.9, 151.7, 143.9, 142.5, 138.7, 137.3, 136.2, 131.7, 129.3, 129.2, 127.5, 127.2, 126.7, 125.9, 125.4, 125.3, 124.8, 124.1, 117.9, 110.2, 96.6, 92.6, 51.6, 34.4, 30.2, 21.7. HRMS (ESI-TOF) calcd. for $C_{36}H_{37}BrN_2O_6SNa$ $[M + Na]^+$ 729.1434; found: 729.1439.

3j, white solid, 31.3 mg, 49% yield; m.p. 193.8–194.9 °C; 1H NMR (400 MHz, Chloroform-*d*) δ 8.16 (d, J = 8.2 Hz, 1H), 7.69–7.62 (m, 3H), 7.37–7.29 (m, 1H), 7.29–7.15 (m, 6H), 7.04 (s, 1H), 6.79 (s, 2H), 6.72 (dd, J = 7.8, 1.7 Hz, 1H), 5.32 (s, 1H), 2.44 (s, 3H), 2.42 (s, 3H), 1.33 (s, 18H). ^{13}C NMR (101 MHz, Chloroform-*d*) δ 154.3, 147.2, 145.8, 136.6, 136.0, 135.0, 132.7, 132.1, 129.9, 129.8, 129.5, 128.9, 128.5, 128.1, 127.4, 126.3, 126.3, 125.4, 122.3, 120.4, 119.2, 111.9, 59.8, 34.4, 30.1, 21.9, 21.7. HRMS (ESI-TOF) calcd. for $C_{37}H_{41}N_2O_6S$ $[M + H]^+$ 641.2680; found: 641.2690.

3k, white solid, 41.8 mg, 69% yield; m.p. 178.6–179.4 °C; 1H NMR (400 MHz, Chloroform-*d*) δ 8.30 (d, J = 8.0 Hz, 1H), 7.83–7.76 (m, 2H), 7.71 (s, 1H), 7.69–7.60 (m, 1H), 7.50–7.27 (m, 6H), 7.24–7.16 (m, 2H), 7.07 (s, 1H), 6.82 (s, 2H), 6.70 (dd, J = 8.2, 1.6 Hz, 1H), 5.35 (s, 1H), 1.33 (s, 18H). ^{13}C NMR (101 MHz, Chloroform-*d*) δ 154.4, 147.1, 136.7, 135.6, 135.5, 134.5, 132.0, 130.1, 129.9, 129.3, 128.8, 128.5, 128.1, 127.5, 126.1, 125.4, 124.8, 124.6, 122.5, 121.4, 120.8, 112.1, 60.0, 34.4, 30.2. HRMS (ESI-TOF) calcd. for $C_{35}H_{36}N_2O_6SNa$ $[M + Na]^+$ 635.2186; found: 635.2197.

3l, white solid, 33.9 mg, 66% yield; m.p. 168.4–169.1 °C; 1H NMR (400 MHz, Chloroform-*d*) δ 8.33 (d, J = 8.1 Hz, 1H), 7.82 (s, 1H), 7.45–7.33 (m, 2H), 7.36–7.25 (m, 2H), 7.20–7.11 (m, 2H), 6.90 (s, 2H), 6.85 (s, 1H), 6.60 (dd, J = 7.8, 1.6 Hz, 1H), 5.38 (s, 1H), 1.89 (s, 3H), 1.36 (s, 18H). ^{13}C NMR (101 MHz, Chloroform-*d*) δ 168.2, 154.5, 148.1, 136.9, 135.5, 130.7, 130.3, 129.5, 128.9, 127.4, 126.4, 126.2, 125.6, 124.7, 124.5, 123.6, 121.3, 121.0, 111.6, 60.6, 34.4, 30.1, 20.3. HRMS (ESI-TOF) calcd. for $C_{31}H_{34}N_2O_5Na$ $[M + Na]^+$ 537.2360; found: 537.2369.

3m, white solid, 19.5 mg, 34% yield; m.p. 167.4–168.1 °C; 1H NMR (400 MHz, Chloroform-*d*) δ 8.31 (dt, J = 8.1, 1.0 Hz, 1H), 7.77 (s, 1H), 7.42–7.27 (m, 4H), 7.24 (dd, J = 8.1, 1.2 Hz, 1H), 7.16 (td, J = 7.6, 1.3 Hz, 1H), 7.02 (s, 1H), 6.89 (s, 2H), 6.63 (dd, J = 7.8,

1.6 Hz, 1H), 5.34 (s, 1H), 1.35 (s, 19H), 1.26 (s, 9H). ^{13}C NMR (101 MHz, Chloroform-*d*) δ 154.5, 150.8, 148.4, 136.6, 135.5, 130.8, 130.4, 129.6, 128.8, 127.5, 126.5, 126.1, 125.7, 124.6, 124.5, 123.3, 121.4, 120.9, 111.7, 83.7, 59.9, 34.4, 30.1, 29.7, 27.4. HRMS (ESI-TOF) calcd. for $\text{C}_{34}\text{H}_{40}\text{N}_2\text{O}_6\text{Na}$ $[\text{M} + \text{Na}]^+$ 595.2779; found: 595.2790.

3n, white solid, 41.2 mg, 64% yield; m.p. 209.4–210.0 °C; ^1H NMR (400 MHz, Chloroform-*d*) δ 8.24 (d, J = 8.0 Hz, 1H), 7.66–7.57 (m, 3H), 7.39–7.17 (m, 5H), 7.09 (dd, J = 9.1, 4.6 Hz, 1H), 6.95 (d, J = 9.3 Hz, 2H), 6.74 (s, 2H), 6.31 (dd, J = 8.7, 3.0 Hz, 1H), 5.30 (s, 1H), 2.36 (s, 3H), 1.27 (s, 18H). ^{13}C NMR (101 MHz, Chloroform-*d*) δ 160.9 (d, J = 248.9 Hz), 154.6, 146.2, 142.8 (d, J = 3.1 Hz), 136.8, 135.4, 134.7 (d, J = 7.1 Hz), 132.3, 130.1, 129.7, 129.0, 128.2, 125.5, 124.9, 124.7, 124.3 (d, J = 8.7 Hz), 121.3, 120.9, 116.6 (d, J = 23.5 Hz), 115.4 (d, J = 25.1 Hz), 112.0, 60.1, 34.4, 30.1, 21.8. HRMS (ESI-TOF) calcd. for $\text{C}_{36}\text{H}_{38}\text{FN}_2\text{O}_6\text{S}$ $[\text{M} + \text{H}]^+$ 645.2429; found: 645.2437.

3o, white solid, 36.9 mg, 56% yield; m.p. 182.4–183.6 °C; ^1H NMR (400 MHz, Chloroform-*d*) δ 8.32 (d, J = 8.0 Hz, 1H), 7.73–7.63 (m, 3H), 7.48–7.21 (m, 5H), 7.17 (d, J = 8.7 Hz, 1H), 7.01 (s, 1H), 6.81 (s, 2H), 6.67 (d, J = 2.6 Hz, 1H), 5.39 (s, 1H), 2.44 (s, 3H), 1.35 (s, 18H). ^{13}C NMR (101 MHz, Chloroform-*d*) δ 154.6, 146.3, 145.6, 136.8, 135.4, 134.0, 133.2, 132.2, 130.1, 130.0, 129.7, 129.0, 128.3, 128.2, 125.4, 125.3, 124.9, 124.7, 123.8, 121.3, 120.9, 111.9, 59.9, 34.4, 30.1, 21.8. HRMS (ESI-TOF) calcd. for $\text{C}_{36}\text{H}_{37}\text{ClN}_2\text{O}_6\text{SNa}$ $[\text{M} + \text{Na}]^+$ 683.1953; found: 683.1961.

3p, white solid, 42.2 mg, 60% yield; m.p. 193.8–195.9 °C; ^1H NMR (400 MHz, Chloroform-*d*) δ 8.32 (d, J = 8.0 Hz, 1H), 7.72–7.62 (m, 3H), 7.49–7.23 (m, 6H), 7.10 (d, J = 8.7 Hz, 1H), 7.00 (s, 1H), 6.82 (d, J = 2.3 Hz, 1H), 6.80 (s, 2H), 5.38 (s, 1H), 2.43 (s, 3H), 1.34 (s, 18H). ^{13}C NMR (101 MHz, Chloroform-*d*) δ 154.6, 146.3, 146.2, 136.8, 135.4, 134.3, 133.0, 132.2, 131.2, 130.1, 129.7, 129.1, 128.2, 125.4, 125.4, 124.9, 124.7, 124.1, 121.3, 120.9, 111.9, 59.8, 3.4, 30.1, 21.8. HRMS (ESI-TOF) calcd. for $\text{C}_{36}\text{H}_{37}\text{BrN}_2\text{O}_6\text{SNa}$ $[\text{M} + \text{Na}]^+$ 729.1434; found: 729.1448.

3q, white solid, 38.0 mg, 54% yield; m.p. 259.8–260.4 °C; ^1H NMR (400 MHz, Chloroform-*d*) δ 8.30 (d, J = 8.0 Hz, 1H), 7.70–7.63 (m, 3H), 7.45–7.37 (m, 2H), 7.37–7.21 (m, 6H), 6.96 (s, 1H), 6.79 (s, 2H), 6.55 (d, J = 8.3 Hz, 1H), 5.37 (s, 1H), 2.44 (s, 3H), 1.33 (s, 18H). ^{13}C NMR (101 MHz, Chloroform-*d*) δ 154.5, 147.2, 146.3, 136.8, 135.4, 132.1, 131.2, 130.6, 130.1, 129.8, 129.5, 128.9, 128.2, 125.8, 125.5, 125.3, 124.9, 124.7, 122.7, 121.3, 120.8, 112.0, 59.8, 34.4, 30.1, 21.8. HRMS (ESI-TOF) calcd. for $\text{C}_{36}\text{H}_{37}\text{BrN}_2\text{O}_6\text{SNa}$ $[\text{M} + \text{Na}]^+$ 729.1434; found: 729.1439.

3r, white solid, 45.4 mg, 71% yield; m.p. 196.3–197.4 °C; ^1H NMR (400 MHz, Chloroform-*d*) δ 8.34–8.27 (m, 1H), 7.72 (s, 1H), 7.69–7.62 (m, 2H), 7.45–7.36 (m, 2H), 7.36–7.20 (m, 4H), 7.11 (dd, J = 8.4, 1.9 Hz, 1H), 7.06 (d, J = 17.7 Hz, 2H), 6.80 (s, 2H), 6.49 (d, J = 1.9 Hz, 1H), 5.33 (s, 1H), 2.42 (s, 3H), 2.21 (s, 3H), 1.33 (s, 18H). ^{13}C NMR (101 MHz, Chloroform-*d*) δ 154.3, 145.8, 145.0, 137.5, 136.6, 135.6, 132.7, 131.5, 130.4, 130.2, 129.9, 128.8, 128.7, 128.2, 126.3, 125.4, 124.7, 124.5, 122.2, 121.3, 120.7, 112.2, 59.9, 34.4, 30.2, 21.8, 21.2. HRMS (ESI-TOF) calcd. for $\text{C}_{37}\text{H}_{40}\text{N}_2\text{O}_6\text{SNa}$ $[\text{M} + \text{Na}]^+$ 663.2499; found: 663.2508.

3s, white solid, 28.9 mg, 44% yield; m.p. 203.5–204.6 °C; ^1H NMR (400 MHz, Chloroform-*d*) δ 8.29 (d, J = 8.0 Hz, 1H), 7.67 (s, 1H), 7.61 (d, J = 8.0 Hz, 2H), 7.44–7.36 (m, 1H), 7.29 (dd, J = 16.3, 9.0 Hz, 2H), 7.19 (d, J = 8.0 Hz, 2H), 6.96 (s, 1H), 6.86 (d, J = 2.5 Hz, 1H), 6.76 (s, 2H), 6.73 (d, J = 2.5 Hz, 1H), 6.65 (d, J = 8.7 Hz, 1H), 5.31 (s, 1H), 3.76 (s, 3H), 2.40 (s, 3H), 1.32 (s, 18H). ^{13}C NMR (101 MHz, Chloroform-*d*) δ 160.5, 154.1, 148.0, 145.9, 136.5, 135.5, 132.4, 130.0, 129.9, 129.6, 128.6, 128.1, 126.7, 124.9, 124.7, 124.5, 123.3, 121.3, 120.7, 112.9, 112.2, 108.3, 59.4, 55.7, 34.4, 30.2, 21.8. HRMS (ESI-TOF) calcd. for $\text{C}_{37}\text{H}_{40}\text{N}_2\text{O}_7\text{SNa}$ $[\text{M} + \text{Na}]^+$ 679.2448; found: 679.2458.

3t, white solid, 48.5 mg, 74% yield; m.p. 216.9–217.6 °C; ^1H NMR (400 MHz, Chloroform-*d*) δ 8.30 (d, J = 8.1 Hz, 1H), 7.87–7.80 (m, 3H), 7.54 (d, J = 8.3 Hz, 1H), 7.43–7.35 (m, 1H), 7.35–7.27 (m, 3H), 7.21 (s, 1H), 7.18–7.08 (m, 1H), 6.90 (s, 3H), 6.31 (dd, J = 8.0, 1.4 Hz, 1H), 5.34 (s, 1H), 3.59 (s, 3H), 2.44 (s, 3H), 1.35 (s, 18H). ^{13}C NMR (101 MHz, Chloroform-*d*) δ 154.4, 152.6, 145.2, 136.7, 136.5, 135.7, 134.6, 134.2, 130.3, 129.5, 128.7, 128.2, 127.9,

126.1, 125.8, 124.7, 124.5, 121.4, 120.7, 119.2, 112.7, 112.5, 60.5, 55.6, 34.4, 30.2, 21.7. HRMS (ESI-TOF) calcd. for $C_{37}H_{40}N_2O_7SNa$ $[M + Na]^+$ 679.2448; found: 679.2455.

3.3. The Experimental Procedure for Synthesis of Compound 6 (Scheme 5)

In a reaction tube equipped with a magnetic stirring bar, the indole-3-carboxylate **5** (0.1 mmol, 1 equiv), *ortho*-tosylaminophenyl *p*-QMs **2** (0.1 mmol, 1.0 equiv), K_2CO_3 (0.2 mmol, 2.0 equiv) and acetonitrile (1.0 mL) were added. Then, the mixture was stirred at room temperature. After completion, the mixture was concentrated and purified by flash chromatography on silica gel (petroleum ether/ethyl acetate = 15/1) to afford **6** in 40% yield.

6, 25.5 mg, 40% yield; 1H NMR (400 MHz, Chloroform-*d*) δ 8.19–8.14 (m, 1H), 7.68–7.62 (m, 2H), 7.48 (s, 1H), 7.31–7.26 (m, 2H), 7.26–7.24 (m, 2H), 7.23–7.21 (m, 1H), 7.21–7.17 (m, 2H), 7.17–7.13 (m, 1H), 6.99 (s, 1H), 6.78 (s, 2H), 6.65 (dd, J = 7.8, 1.6 Hz, 1H), 5.27 (s, 1H), 3.88 (s, 3H), 2.41 (s, 3H), 1.32 (s, 18H). ^{13}C NMR (101 MHz, Chloroform-*d*) δ 165.7, 153.9, 147.2, 145.6, 136.9, 136.2, 133.6, 132.9, 132.8, 129.9, 129.4, 128.7, 128.1, 127.3, 127.2, 126.9, 125.5, 122.9, 122.2, 122.1, 121.5, 111.4, 107.1, 59.3, 51.0, 34.3, 30.2, 21.7. HRMS (ESI-TOF) calcd. for $C_{38}H_{41}NO_6SNa$ $[M + Na]^+$ 662.2547; found: 662.2553.

3.4. The Experimental Procedure for Synthesis of Compound 11 (Scheme 5)

In a reaction tube equipped with a magnetic stirring bar, the 3-nitroindoles **1** (0.1 mmol, 1 equiv), *ortho*-OMe phenyl *p*-QM **10** (0.1 mmol, 1.0 equiv), K_2CO_3 (0.2 mmol, 2.0 equiv), PhOH (1.0 mmol, 1.0 equiv) and acetonitrile (1.0 mL) were added. Then, the mixture was stirred at room temperature. After completion, the mixture was concentrated and purified by flash chromatography on silica gel to give the corresponding product **11**.

11, white solid, 9.7 mg, 20% yield; m.p. 227.4–228.2 °C; 1H NMR (400 MHz, Chloroform-*d*) δ 8.30 (d, J = 8.1 Hz, 1H), 7.83 (s, 1H), 7.43–7.22 (m, 4H), 7.10 (s, 1H), 6.99–6.89 (m, 4H), 6.78 (dd, J = 7.7, 1.7 Hz, 1H), 5.30 (s, 1H), 3.77 (s, 3H), 1.35 (s, 18H). ^{13}C NMR (101 MHz, Chloroform-*d*) δ 156.7, 154.0, 136.4, 135.7, 130.4, 130.0, 128.6, 128.4, 127.1, 126.4, 125.1, 124.3, 124.3, 121.4, 120.9, 120.8, 111.9, 111.0, 59.2, 55.7, 34.4, 30.2. HRMS (ESI-TOF) calcd. for $C_{30}H_{34}N_2O_4Na$ $[M + Na]^+$ 509.2411; found: 509.2419.

4. Conclusions

In conclusion, we have described an unprecedented *N*-alkylation of 3-nitroindoles and *para*-quinone methides by using K_2CO_3 as the base via a protection group migration/*aza*-1,6-Michael addition sequences. With the developed protocol, a series of structurally diverse *N*-diarylmethylindole derivatives were obtained in moderate to good yields under mild conditions. According to the control experiments, a reasonable reaction mechanism was proposed. Importantly, the reaction herein is featured that 3-nitroindoles is defined with latent *N*-centered nucleophiles to react with *ortho*-hydrophenyl *p*-QMs, which is different from the previous reports where 3-nitroindoles was served as electrophiles trapped by various nucleophiles.

Supplementary Materials: The following supporting information can be downloaded at: <https://www.mdpi.com/article/10.3390/molecules28145529/s1>, X-ray data for products **3l** and **3p**; copies of 1H and ^{13}C NMR spectra.

Author Contributions: Conceptualization, J.-Q.Z. and W.-C.Y.; methodology, W.-J.W., S.Z. and Q.-L.X.; investigation, X.-S.X., Y.-P.Z., Y.Y. and Z.-H.W.; writing—original draft preparation, J.-Q.Z.; writing—review and editing, J.-Q.Z. and W.-C.Y.; supervision, J.-Q.Z. and W.-C.Y. All authors have read and agreed to the published version of the manuscript.

Funding: This research was funded by the Natural Science Foundation of China, grant number 22271027, 22171029 and 21901024; the Sichuan Science and Technology Program, grant number 2021YFS0315; and the Talent Program of Chengdu University, grant number 2081919035, 2081921038.

Institutional Review Board Statement: Not applicable.

Informed Consent Statement: Not applicable.

Data Availability Statement: All the required data are reported in the manuscript and Supplementary Materials.

Acknowledgments: This work was performed using the equipment of Chengdu University and Chengdu Institute of Organic Chemistry, Chinese Academy of Sciences.

Conflicts of Interest: The authors declare no conflict of interest.

Sample Availability: Samples of the compounds are available from the authors upon request.

References

1. Somei, M.; Yamada, F. Simple indole alkaloids and those with a non-rearranged monoterpenoid unit. *Nat. Prod. Rep.* **2005**, *22*, 73–103. [\[CrossRef\]](#) [\[PubMed\]](#)
2. de Sa Alves, F.R.; Barreiro, E.J.; Fraga, C.A.M. From Nature to Drug Discovery: The Indole Scaffold as a ‘Privileged Structure’. *Mini-Rev. Med. Chem.* **2009**, *9*, 782–793. [\[CrossRef\]](#)
3. Kochanowska-Karamyan, A.J.; Hamann, M.T. Marine indole alkaloids: Potential new drug leads for the control of depression and anxiety. *Chem. Rev.* **2010**, *110*, 4489–4497. [\[CrossRef\]](#)
4. Sravanthi, T.V.; Manju, S.L. Indoles—A Promising Scaffold for Drug Development. *Eur. J. Pharm. Sci.* **2016**, *91*, 1–10. [\[CrossRef\]](#) [\[PubMed\]](#)
5. Chadha, N.; Silakari, O. Indoles as therapeutics of interest in medicinal chemistry: Bird’s eye view. *Eur. J. Med. Chem.* **2017**, *134*, 159–184. [\[CrossRef\]](#) [\[PubMed\]](#)
6. Wan, Y.; Li, Y.; Yan, C.; Yan, M.; Tang, Z. Indole: A privileged scaffold for the design of anti-cancer agents. *Eur. J. Med. Chem.* **2019**, *183*, 111691. [\[CrossRef\]](#) [\[PubMed\]](#)
7. Humphrey, G.R.; Kuethe, J.T. Practical Methodologies for the Synthesis of Indoles. *Chem. Rev.* **2006**, *106*, 2875–2911. [\[CrossRef\]](#)
8. Bandini, M.; Eichholzer, A. Catalytic Functionalization of Indoles in a New Dimension. *Angew. Chem. Int. Ed.* **2009**, *48*, 9608–9644. [\[CrossRef\]](#)
9. Bartoli, G.; Bencivenni, G.; Dalpozzo, R. Organocatalytic strategies for the asymmetric functionalization of indoles. *Chem. Soc. Rev.* **2010**, *39*, 4449–4465. [\[CrossRef\]](#)
10. Dalpozzo, R. Strategies for the asymmetric functionalization of indoles: An update. *Chem. Soc. Rev.* **2015**, *44*, 742–778. [\[CrossRef\]](#)
11. Sheng, F.-T.; Wang, J.-Y.; Tan, W.; Zhang, Y.-C.; Shi, F. Progresses in organocatalytic asymmetric dearomatization reactions of indole derivatives. *Org. Chem. Front.* **2020**, *7*, 3967–3998. [\[CrossRef\]](#)
12. Zhang, H.-H.; Shi, F. Organocatalytic Atroposelective Synthesis of Indole Derivatives Bearing Axial Chirality: Strategies and Applications. *Acc. Chem. Res.* **2022**, *55*, 2562–2580. [\[CrossRef\]](#) [\[PubMed\]](#)
13. You, S.-L.; Cai, Q.; Zeng, M. Chiral Brønsted acid catalyzed Friedel–Crafts alkylation reactions. *Chem. Soc. Rev.* **2009**, *38*, 2190–2201. [\[CrossRef\]](#)
14. Sandtorv, A.H. Transition Metal-Catalyzed C–H Activation of Indoles. *Adv. Synth. Catal.* **2015**, *357*, 2403–2435. [\[CrossRef\]](#)
15. Trubitsin, D.; Kanger, T. Enantioselective Catalytic Synthesis of *N*-alkylated Indoles. *Symmetry* **2020**, *12*, 1184. [\[CrossRef\]](#)
16. Ma, J.; Feng, R.; Dong, Z.-B. Recent Advances in Indole Synthesis and the Related Alkylation. *Asian J. Org. Chem.* **2023**, *12*, e202300092. [\[CrossRef\]](#)
17. Chen, M.; Sun, J. Catalytic Asymmetric *N*-Alkylation of Indoles and Carbazoles through 1,6-Conjugate Addition of Aza-paraquinone Methides. *Angew. Chem. Int. Ed.* **2017**, *56*, 4583–4587. [\[CrossRef\]](#) [\[PubMed\]](#)
18. Zhang, L.; Wu, B.; Chen, Z.; Hu, J.; Zeng, X.; Zhong, G. Chiral phosphoric acid catalyzed enantioselective *N*-alkylation of indoles with in situ generated cyclic *N*-acyl ketimines. *Chem. Commun.* **2018**, *54*, 9230–9233. [\[CrossRef\]](#)
19. Allen, J.R.; Bahamonde, A.; Furukawa, Y.; Sigman, M.S. Enantioselective *N*-Alkylation of Indoles via an Intermolecular Aza-Wacker-Type Reaction. *J. Am. Chem. Soc.* **2019**, *141*, 8670–8674. [\[CrossRef\]](#)
20. Gnanamani, E.; Yan, X.; Zare, R.N. Chemoselective *N*-Alkylation of Indoles in Aqueous Microdroplets. *Angew. Chem. Int. Ed.* **2020**, *59*, 3069–3072. [\[CrossRef\]](#)
21. Clanton, N.A.; Spiller, T.E.; Ortiz, E.; Gao, Z.; Rodriguez-Poirier, J.M.; DelMonte, A.J.; Frantz, D.E. A Metal-Free Reductive *N*-Alkylation of Indoles with Aldehydes. *Org. Lett.* **2021**, *23*, 3233–3236. [\[CrossRef\]](#) [\[PubMed\]](#)
22. Yang, S.; Li, L.; Zhao, J. Chiral Phosphoric Acid-Catalyzed Chemo- and Enantioselective *N*-Alkylation of Indoles with Imines. *Adv. Syn. Catal.* **2022**, *364*, 4166–4172. [\[CrossRef\]](#)
23. Zha, T.; Rui, J.; Zhang, Z.; Zhang, D.; Yang, Z.; Yu, P.; Wang, Y.; Peng, F.; Shao, Z. Direct Catalytic Asymmetric and Regiodivergent *N*1-and C3-Allelylic Alkylation of Indoles. *Angew. Chem. Int. Ed.* **2023**, *62*, e202300844. [\[CrossRef\]](#) [\[PubMed\]](#)
24. Shaw, M.H.; Shurtleff, V.W.; Terrett, J.A.; Cuthbertson, J.D.; MacMillan, D.W.C. Native functionality in triple catalytic cross-coupling: sp³ C–H bonds as latent nucleophiles. *Science* **2016**, *352*, 1304–1308. [\[CrossRef\]](#) [\[PubMed\]](#)
25. Geri, J.B.; Wade Wolfe, M.M.; Szymczak, N.K. The Difluoromethyl Group as a Masked Nucleophile: A Lewis Acid/Base Approach. *J. Am. Chem. Soc.* **2018**, *140*, 9404–9408. [\[CrossRef\]](#)
26. Lange, M.; Zi, Y.; Vilotijevic, I. Enantioselective Synthesis of Pyrrolizin-1-ones via Lewis Base Catalyzed *N*-Allylation of *N*-Silyl Pyrrole Latent Nucleophiles. *J. Org. Chem.* **2020**, *85*, 1259–1269. [\[CrossRef\]](#)

27. Kumar, S.; Lange, M.; Zi, Y.; Görls, H.; Vilotijevic, I. Latent Pronucleophiles in Lewis Base Catalysis: Enantioselective Allylation of Silyl Enol Ethers with Allylic Fluorides. *Chem. Eur. J.* **2023**, *29*, e202300641. [\[CrossRef\]](#)
28. Zi, Y.; Lange, M.; Schultz, C.; Vilotijevic, I. Latent Nucleophiles in Lewis Base Catalyzed Enantioselective *N*-Allylation of *N*-Heterocycles. *Angew. Chem. Int. Ed.* **2019**, *58*, 10727–10731. [\[CrossRef\]](#)
29. Cerveri, A.; Bandini, M. Recent Advances in the Catalytic Functionalization of “Electrophilic” Indoles. *Chin. J. Chem.* **2020**, *38*, 287–294. [\[CrossRef\]](#)
30. Rkein, B.; Bigot, A.; Birbaum, L.; Manneveau, M.; De Paolis, M.; Legros, J.; Chataigner, I. Reactivity of 3-nitroindoles with electron-rich species. *Chem. Commun.* **2021**, *57*, 27–44. [\[CrossRef\]](#)
31. Nair, S.R.; Baire, B. Recent Dearomatization Strategies of Benzofurans and Benzothiophenes. *Asian J. Org. Chem.* **2021**, *10*, 932–948. [\[CrossRef\]](#)
32. Wang, N.; Ren, J.; Li, K. Dearomatization of Nitro(hetero)arenes through Annulation. *Eur. J. Org. Chem.* **2022**, *2022*, e202200039. [\[CrossRef\]](#)
33. Li, Y.-L.; Wang, K.-K.; He, X.-L. Recent Progress of Electron-Withdrawing-Group-Tethered Arenes Involved Asymmetric Nucleophilic Aromatic Functionalizations. *Adv. Synth. Catal.* **2022**, *364*, 3630–3650. [\[CrossRef\]](#)
34. Jaworski, A.A.; Scheidt, K.A. Emerging Roles of in situ Generated Quinone Methides in Metal-Free Catalysis. *J. Org. Chem.* **2016**, *81*, 10145–10153. [\[CrossRef\]](#) [\[PubMed\]](#)
35. Li, W.; Xu, X.; Zhang, P.; Li, P. Recent Advances in the Catalytic Enantioselective Reactions of *para*-Quinone Methides. *Chem.-Asian J.* **2018**, *13*, 2350–2359. [\[CrossRef\]](#)
36. Wang, J.-Y.; Hao, W.-J.; Tu, S.-J.; Jiang, B. Recent Developments in 1,6-Addition Reactions of *para*-Quinone Methides (*p*-QMs). *Org. Chem. Front.* **2020**, *7*, 1743–1778. [\[CrossRef\]](#)
37. Wang, D.; Sun, J.; Yan, C.-G. Diastereoselective Synthesis of Spiro[chromane-3,3'-indolines] and Spiro[chromane-3,2'-indenes] via DBU Promoted Formal [4 + 2] Cycloaddition Reaction. *Green Synth. Catal.* **2022**, *3*, 53–58. [\[CrossRef\]](#)
38. Zhao, K.; Zhi, Y.; Shu, T.; Valkonen, A.; Rissanen, K.; Enders, D. Organocatalytic Domino Oxa-Michael/1,6-Addition Reactions: Asymmetric Synthesis of Chromans Bearing Oxindole Scaffolds. *Angew. Chem. Int. Ed.* **2016**, *55*, 12104–12108. [\[CrossRef\]](#)
39. Jiang, X.-L.; Wu, S.-F.; Wang, J.-R.; Mei, G.-J.; Shi, F. Catalytic Asymmetric [4 + 2] Cyclization of *para*-Quinone Methide Derivatives with 3-Alkyl-2-vinylindoles. *Adv. Syn. Catal.* **2018**, *360*, 4225–4235. [\[CrossRef\]](#)
40. Xiang, M.; Li, C.-Y.; Song, X.-J.; Zou, Y.; Huang, Z.-C.; Li, X.; Tian, F.; Wang, L.-X. Organocatalytic and enantioselective [4 + 2] cyclization between hydroxymaleimides and *ortho*-hydroxyphenyl *para*-quinone methide-selective preparation of chiral hemiketals. *Chem. Commun.* **2020**, *56*, 14825–14828. [\[CrossRef\]](#)
41. You, Y.; Li, T.-T.; Yuan, S.-P.; Xie, K.-X.; Wang, Z.-H.; Zhao, J.-Q.; Zhou, M.-Q.; Yuan, W.-C. Catalytic asymmetric [4 + 2] cycloaddition of 1-((2-aryl)vinyl)naphthalen-2-ols with in situ generated *ortho*-quinone methides for the synthesis of polysubstituted chromanes. *Chem. Commun.* **2020**, *56*, 439–442. [\[CrossRef\]](#) [\[PubMed\]](#)
42. Chen, G.; Li, H.; Liang, G.; Pu, Q.; Bai, L.; Zhang, D.; Ye, Y.; Li, Y.; Zhou, J.; Zhou, H. Facile construction of dibenzodioxo[3.3.1]nonanes bearing spirocyclohexadienones via domino [4 + 2] cycloaddition/C(sp³)-H oxidative dehydrogenation coupling reactions. *Org. Biomol. Chem.* **2022**, *20*, 9392–9396. [\[CrossRef\]](#) [\[PubMed\]](#)
43. Li, J.; Xi, W.; Liu, S.; Yang, Y.; Yang, J.; Ding, H.; Wang, Z. HFIP-catalyzed highly diastereoselective formal [4 + 2] cyclization to synthesize difluorinated multisubstituted chromans using difluoroenoxy silanes as C2 synthons. *Chin. Chem. Lett.* **2022**, *33*, 3007–3011. [\[CrossRef\]](#)
44. Li, H.-H.; Meng, Y.-N.; Chen, C.-M.; Wang, Y.-Q.; Zhang, Z.-X.; Xu, Z.; Zhou, B.; Ye, L.-W. Chiral Brønsted acid-catalyzed asymmetric intermolecular [4 + 2] annulation of ynamides with *para*-quinone methides. *Sci. China Chem.* **2023**, *66*, 1467–1473. [\[CrossRef\]](#)
45. Zhao, J.-Q.; Zhou, S.; Wang, Z.-H.; You, Y.; Chen, S.; Liu, X.-L.; Zhou, M.-Q.; Yuan, W.-C. Catalytic asymmetric dearomative [4 + 2] annulation of 2-nitrobenzofurans and 5H-thiazol-4-ones: Stereoselective construction of dihydrobenzofuran-bridged polycyclic skeletons. *Org. Chem. Front.* **2021**, *8*, 6330–6336. [\[CrossRef\]](#)
46. Zhao, J.-Q.; Zhou, S.; Qian, H.-L.; Wang, Z.-H.; Zhang, Y.-P.; You, Y.; Yuan, W.-C. Higher-order [10 + 2] cycloaddition of 2-alkylidene-1-indanones enables the dearomatization of 3-nitroindoles: Access to polycyclic cyclopenta[*b*]indoline derivatives. *Org. Chem. Front.* **2022**, *9*, 3322–3327. [\[CrossRef\]](#)
47. Zhou, X.-J.; Zhao, J.-Q.; Lai, Y.-Q.; You, Y.; Wang, Z.-H.; Yuan, W.-C. Organocatalyzed asymmetric dearomative 1,3-dipolar cycloaddition of 2-nitrobenzofurans and *N*-2,2,2-trifluoroethylisatin ketimines. *Chirality* **2022**, *34*, 1019–1034. [\[CrossRef\]](#)
48. Yuan, W.-C.; Chen, X.-M.; Zhao, J.-Q.; Zhang, Y.-P.; Wang, Z.-H.; You, Y. Ag-Catalyzed Asymmetric Interrupted Barton-Zard Reaction Enabling the Enantioselective Dearomatization of 2- and 3-Nitroindoles. *Org. Lett.* **2022**, *24*, 826–831. [\[CrossRef\]](#)
49. Zhou, S.; Qian, H.-L.; Zhao, J.-Q.; You, Y.; Wang, Z.-H.; Yin, J.-Q.; Zhang, Y.-P.; Chen, M.-F.; Yuan, W.-C. Diastereoselective synthesis of polycyclic indolines via dearomative [4 + 2] cycloaddition of 3-nitroindoles with *ortho*-aminophenyl *p*-quinone methides. *Org. Biomol. Chem.* **2023**, *21*, 1373–1378. [\[CrossRef\]](#)

Disclaimer/Publisher's Note: The statements, opinions and data contained in all publications are solely those of the individual author(s) and contributor(s) and not of MDPI and/or the editor(s). MDPI and/or the editor(s) disclaim responsibility for any injury to people or property resulting from any ideas, methods, instructions or products referred to in the content.